Article

Journal of the Brazilian Chemical Society

https://dx.doi.org/10.21577/0103-5053.20230178

J. Braz. Chem. Soc., Vol. 00, No. 00, e-20230178, 1-10, 2023

Is Natural Solar Photolysis Effective for the Removal of Antibiotics and Pathogens from Waste Stabilization Pond?

Karla V. L. Lima,[a] *Jany H. F. de Jesus,*[#,a] *João L. Bronzel Junior*[a] *and Raquel F. P. Nogueira*[*,a]

[a]*Instituto de Química, Universidade Estadual Paulista (UNESP), 14800-060 Araraquara-SP, Brazil*

This study aimed to investigate the occurrence of photolysis of two relevant antibiotics, sulfamethoxazole and trimethoprim, when present in a Waste Stabilization Pond and its disinfection under tropical irradiance. The influence of pH and matrix components, and the generation of photoproducts during solar exposure were evaluated. The pH-dependent speciation of antibiotics had a greater influence on the photolysis of antibiotics than the water matrix, with higher photodegradation at pH 4.1 than at pH 7.2. Trimethoprim was more susceptible to indirect photolysis, indicated by the steeper influence of the photosensitizers nitrate and humic acid compared to sulfamethoxazole. The photoproducts generated were persistent to photolysis and remained present in the samples up to 70 h irradiation. Wastewater disinfection was achieved after 70 h of solar exposure. Nonetheless, the exposure time required to remove at least 50% of sulfamethoxazole was on average 29 h and of trimethoprim 83 h, at the natural pH of the matrix (pH 7.2). Given that the residence time in Waste Stabilization Pond is 41 h, which corresponds to a maximum of 26 h solar irradiation, the exposure time in Waste Stabilization Pond is not sufficient to completely photodegrade antibiotics or disinfect the effluent, demanding further treatment.

Keywords: trimethoprim, sulfamethoxazole, photodegradation, wastewater treatment plant, nitrate, humic acid

Introduction

Waste Stabilization Ponds (WSPs) are applied in Wastewater Treatment Plants (WWTPs) based on a natural biological process. In this system, the wastewater remains in large open ponds for hours or days, while microorganisms metabolize organic matter and remove pathogens as well as nutrients such as nitrogen and phosphorus.[1] The use of WSPs is a cost-effective and low-maintenance technology that does not require any energy input or specialized labor for operation. Additionally, the use of wastewater treatment systems by WSPs is an advantageous option, as they are considered more robust and can have greater energy and treatment efficiencies in warmer climates.[1-3]

Mechanisms such as hydrolysis, photodegradation and biodegradation may occur in WSPs during the residence time and contribute to the removal of pharmaceuticals and other substances from the aqueous matrix.[1] Among them, photolysis can have the greatest contribution to the removal of contaminants in tropical regions due to the high solar irradiance that reaches the surface while this process can be facilitated in the presence of photosensitizers in aqueous medium. In addition, photolysis is an alternative way to degrade toxic compounds that are not degraded by biological processes, as well as in the case of molecules which do not undergoe hydrolysis.[4]

Photolysis of contaminants in an aqueous medium may occur either by photon absorption leading to the cleavage of chemical bonds (direct photolysis) or via reactive oxygen species (ROS) formed during the absorption of radiation by photosensitizers present in the medium (indirect photolysis) resulting in contaminant degradation. The composition of a typical WSP matrix, with the presence of dissolved organic matter (DOM) and inorganic species such as nitrate, plays an important role during the photolysis process. Nitrate can serve as a source of HO$^{\bullet}$ under irradiation, thereby promoting the indirect photolysis of organic contaminants. On the other hand, DOM can exhibit both inhibitory and promoting effects on photolysis. The absorption of radiation by DOM can lead to the formation of ROS, such as HO$^{\bullet}$, singlet oxygen

*e-mail: raquel.pupo@unesp.br
#Present address: Instituto de Química, Universidade de São Paulo (USP), 05508-000 São Paulo-SP, Brazil
Editor handled this article: Maria Cristina Canela (Associate)

($^1O_2$), superoxide (O^{2-}), hydrogen peroxide (H_2O_2), excited singlet-state DOM (^{1}DOM*), and excited triplet-state DOM (^{3}DOM*), all of which contribute to indirect photolysis. However, DOM can also compete for photons and quench the formed species, reducing the photolysis.[4-6]

Most studies on the occurrence of photolysis in different matrices are performed under simulated solar irradiation.[7-13] To better understand micro-contaminant behavior in the environment, the study of the occurrence of reactions under natural conditions is very important. Studies performed in the laboratory using simulated solar irradiation do not consider daily and seasonal variations in solar intensity, which directly affect the photolysis of the compounds. In addition, most of the available photochemical studies are biased toward temperate and subarctic regions, and more attention needs to be paid to the tropics where incident solar irradiation is more intense.[4]

Brazil has an average daily global horizontal irradiation value above 5 kWh m^{-2} *per* day for some regions, representing a much higher solar incidence than European countries.[14] In addition, Brazil treats a great part of the sewage generated in WSP systems[15] and the high incidence of solar irradiation may contribute to the removal of aqueous contaminants as antibiotics. The occurrence of antibiotics in Brazilian surface waters has been widely reported in several studies.[16-19] The contribution of residues of antibiotics to the spread of resistant bacteria and genes is one of the biggest concerns about the presence of these substances in water systems, which certainly involves a serious risk to human health and has attracted particular attention.[20-23]

Thus, this study investigated the photolysis of two antibiotics sulfamethoxazole (SMX) and trimethoprim (TMP), which are often used in combination to treat a wide variety of bacterial infections, in Brazilian WSP samples under natural solar irradiation. The objective was to evaluate the contribution of this natural process in the removal of these antibiotics during their residency time at WWTP under tropical irradiance. The effect of nitrate (NO_3^-), humic acid (HA), matrix and pH, were evaluated. Furthermore, the elimination of pathogens and the main photoproducts formed during the natural solar photolysis process were also evaluated.

Experimental

Chemicals

Sulfamethoxazole (≥ 98%), trimethoprim (99.8%), and humic acid (HA) were acquired from Sigma-Aldrich (Saint Louis, USA). Sodium nitrate ($NaNO_3$, 99%) was purchased from Mallinckrodt (Saint Louis, USA). Formic acid (88%) and isopropanol (high performance liquid chromatography (HPLC) grade) were obtained from J.T. Baker (Phillipsburg, USA). Sodium hydroxide (NaOH, 98%) and sulfuric acid (95-98%) were obtained from Synth (São Paulo, Brazil). Methanol (HPLC grade) was purchased from Supelco (Darmstadt, Germany). Ultrapure Millipore Milli Q water (Direct-Q® Water Purification System, Merck, Darmstadt, Germany) was used to prepare stock solutions.

Water matrices

The photolysis experiments were performed in ultrapure water and WSP samples. The WSP samples were collected from the stabilization ponds of the WWTP in Araraquara (21°49'28.3"S 48°15'07.5"W), São Paulo, Brazil, where the urban wastewater is subjected to primary and secondary treatment composed of aeration and sedimentation ponds.[24]

Samples of the WSP were collected in July-October 2021 between winter and spring in the dry season. The samples were collected in amber flasks, vacuum filtered using 80 g blue dot quantitative filter paper and stored at 4 ºC for up to two weeks. Before all photolysis experiments, the effluent was also filtered with cellulose acetate membrane (0.45 µm pore size) and spiked with 500 µg L^{-1} of each antibiotic. The main physical and chemical parameters determined for the WSP effluent are shown in Table S1 (Supplementary Information (SI) section).

Photolysis experiments

Photolysis experiments were performed in quartz tubes (outer diameter = 23 mm, internal diameter = 20 mm, volume = 45 mL) to ensure adequate sunlight penetration. The tubes containing a solution of the antibiotics SMX and TMP (500 µg L^{-1} of each) were horizontally exposed to natural solar irradiation between 8 a.m. and 4 p.m. and conditioned in a plastic tray containing water and artificial ice packs to prevent temperature increase (Figure S1, SI section). Under these conditions, the temperature was maintained at 30 ± 3 °C. At predetermined periods, the solutions were homogenized, and the tubes opened quickly to withdraw 500 µL aliquots, which were analyzed by HPLC using a diode array detector (DAD), as described in the "Analytical methods" sub-section.

At the end of each day, the tubes were stored in a refrigerator protected from light and returned to irradiation exposure on the following day after reaching room temperature. In parallel to the solar photolysis experiment, a control experiment was carried out, in which the antibiotic

solutions were left in the same conditions but in amber flasks in the dark.

The effect of pH was evaluated in the WSP samples at pH 4.1 and pH 7.2 (without adjustment). Sulfuric acid (0.5 mol L^{-1}) and sodium hydroxide (1.0 mol L^{-1}) were used to adjust the pH of the solutions immediately before the experiments.

The effect of natural water constituents was evaluated with the addition of HA (143 mg L^{-1}), that corresponds to 53 mg L^{-1} of total organic carbon (TOC), and NO_3^- (10 mg L^{-1}) in ultrapure water. These concentrations were chosen considering the average concentration of these components in the WSP matrix (Table S1, SI section). The occurrence of indirect photolysis was evaluated by the addition of isopropanol (10 mmol L^{-1}) to scavenge hydroxyl radicals in WSP samples.

Kinetic constants for the photolysis of antibiotics were calculated using both first and second-order equations, to determine the best model, as defined in equations 1 and 2:

$$\ln C = \ln C_0 - kt \quad (1)$$

$$\frac{1}{C} = \frac{1}{C_0} + kt \quad (2)$$

where k is the rate constant (h^{-1}), t is irradiation time, C is the concentration of each antibiotic at a given irradiation time and C_0 is the initial concentration. Data on k constant, determination coefficient (R^2) and half-life time, $t_{1/2}$ (h), obtained for SMX and TMP were also calculated.

For the investigation of the photoproducts generated, a solution of each antibiotic separately (ultrapure water, pH 7.2) was allowed to stay under natural solar irradiation. Solid-phase extraction using Oasis HLB cartridges (3 mL, 60 mg) (Waters Corp., Milford, MA, USA) was performed to pre-concentrate the antibiotics and improve the detection of photoproducts in a procedure according to a previous study.[25]

The UVA dose accumulated during exposure to solar irradiation was measured using a model PMA 2100 Dual-Input Data Logging radiometer (Solar Light Co, Glenside, USA) with a UVA sensor (320-400 nm) positioned horizontally. The photolysis of the drugs was evaluated by the decay of their concentration as a function of the accumulated irradiation dose. The aliquots were taken after 0, 250, 500, 750, 1000, 2000, 3000, 4000, 5000, and 6000 kJ m^{-2}, which corresponds to an average solar exposure of 5.5 h *per* day during 14 days of experimentation.

For effluent disinfection evaluation regarding *Escherichia coli* and total and thermotolerant coliforms, the membrane filtration method described in American Public Health Association (APHA)[26] with a limit of quantification (LOQ) of 1 colony forming units (CFU) *per* 100 mL was applied. Analyses were performed on WSP samples before irradiation, at the meantime of the experiment (after an accumulated UV dose of 3000 kJ m^{-2}), and at the end of the experiment (after 6000 kJ m^{-2}), besides on control samples that remained in the dark.

All experiments were run at least in duplicate. Standard deviations are shown for experiments run in triplicate.

Analytical methods

HPLC using a Prominence LC 20AT instrument (Shimadzu, Kyoto, Japan), equipped with a DAD (SPD-M20) was employed to measure SMX and TMP concentration. A Luna® Omega polar C18 analytical column (100 Å; 150 mm × 4.6 mm; 5 µm; Phenomenex, Torrance, USA) was used at 40 °C for separation at a flow rate of 0.8 mL min^{-1}. The DAD was set at 270 nm, the injection volume was 40 µL and the mobile phase consisted of 0.1% formic acid in water/methanol (75:25) in an isocratic elution. Calibration curves were prepared in both water and WSP samples to evaluate potential matrix effects by comparing the slopes of the two curves. No significant differences were observed in the slopes of the curves, indicating negligible matrix effect (Table S2, SI section). The retention time of TMP and SMX were 5.99 ± 0.02 and 10.53 ± 0.03 min, respectively. Under these conditions, the limit of detection (LOD) was 7 µg L^{-1} for TMP and SMX, and the LOQ were 22 and 23 µg L^{-1} for TMP and SMX, respectively (Table S2, SI section). For simplicity, a concentration below LOD (> 98% degradation) was referred to as fully degraded in the discussion.

High-performance liquid chromatography-electrospray ionization-ion trap-mass spectrometry (HPLC-ESI-IT-MS) was used to identify photoproducts. Liquid chromatography-mass spectrometry (LC-MS/MS) analysis was performed in a Prominence® (Shimadzu, Kyoto, Japan) modular chromatograph consisting of two LC-20AD pumps, a DGU-20A3R degasser unit, a SIL-20A autosampler, a CTO-20A column compartment, an SPD-M20A PDA detector, and a CBM-20A controller, coupled to an Amazon® ESI-IT-MSn mass spectrometer (Bruker, Bremen, Germany). Chromatographic separation was conducted using the same conditions described previously but with an injection volume of 5 and 10 µL for TMP and SMX, respectively.

Mass spectrometry data were acquired in Auto MS/MS enhanced resolution at positive and negative modes, with an acquisition range of mass to charge ratio (*m/z*) between 50-500. Mass spectra were generated by the average of

3 acquired single spectra with a maximum accumulation time of 200 ms and ion target control set at 10^5. Ion source parameters were set as follows: transfer capillary voltage at –4500 for positive mode, +4500 for negative mode, and end plate offset at 500 V for both polarities; nebulizer gas (N_2) pressure at 50.0 psi; drying N_2 flow at 10 L min^{-1} and temperature at 300 °C, respectively. MS^2 acquisitions were performed in enhanced smart fragmentation mode in which the number of precursor ions to be fragmented was set to 3 with an isolation threshold at 50000 ion counts. Helium was used as collision gas in ion trap collision-induced dissociation (CID). The isolation width of precursor ions was set to 3.0 *m/z*; fragmentation intensity was adjusted to 90% with amplitude voltages ramping from 0.4 to 4.0 V *per* fragmentation cycle of 20 ms.

Results and Discussion

Effect of pH

The pH can directly influence the speciation of antibiotics by changing characteristics such as molar absorptivity and maximum absorption wavelength.[27,28] It can also alter the availability and speciation of components in the matrix itself.[29] Thus, experiments were conducted to investigate the influence of pH on the photolysis of both antibiotics.

The photolysis of the two antibiotics was affected by the pH of the medium (Figure 1). This result is in agreement with previous studies,[27,28,30,31] and is related to the influence of pH on the mole fraction variation of the antibiotic species and their characteristics.

A strong effect was observed on SMX photolysis due to the pH change from 4.1 to 7.2, which decreased from total removal to 40% after 2000 kJ m^{-2} accumulated UV dose. Evaluating the absorption spectrum (Figure S2a, SI section), it is possible to notice an increase in the absorption intensity of SMX when the pH decreases from 7.2 to 4.1, which influences the direct photolysis process. These results are in agreement with that found by Boreen *et al.*[27] who studied the photochemical fate of sulfonamides in the aquatic environment and demonstrated that in addition to the increase in the maximum wavelength at higher pH, a change in the magnitude of absorption at wavelengths above 300 nm would affect the photon absorption rate when exposed to solar irradiation.

According to the speciation diagram of SMX (Figure S3a, SI section), at pH 4.1 SMX is in its neutral form (HSMX = 97.7%), which is more photosensitive and susceptible to photochemical degradation, resulting in faster degradation rate than the anionic and cationic species.[27] The increase of pH from 4.1 to 7.2 causes an almost total conversion from the more photosensitive species to the negatively charged species (SMX^- = 96.6%), which is the most stable species to photoreactions and therefore most resistant to photolysis.[27]

The influence of pH on the photodegradation of TMP was less significant, but it was still possible to observe higher photolysis at pH 4.1. As in SMX, the absorbance spectrum of TMP was also influenced by the pH (Figure S2b, SI section) showing lower absorption at pH 7.2. The drop in photolysis of TMP was from 63% at pH 4.1 to 53% at pH 7.2.

The speciation diagram of TMP (Figure S3b, SI section) shows that at pH 4.1 the protonated species is predominant ($HTMP^+$ = 87.8% and H_2TMP^{2+} = 12.0%). At pH 7.2, the mole fraction of the protonated species decreases to 25.2% and there is an increase in the concentration of the neutral TMP species to 74.8%, which is less susceptible to photolysis due to lower molar absorption coefficients than the protonated species.[28,32] However, unlike SMX, at pH 4.1 total conversion of TMP species is not obtained. For the TMP, the mixture of species more and less susceptible to photolysis results in a less important effect of pH on its photolysis compared to SMX.

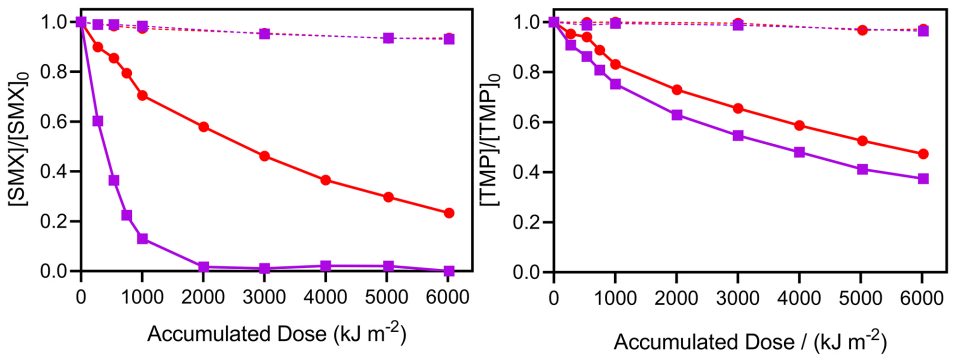

Figure 1. Effect of pH 4.1 (-■-) and pH 7.2 (-●-) on SMX and TMP solar photolysis in Waste Stabilization Pond samples. Dashed lines: dark control experiments. Conditions: 500 µg L^{-1} of SMX and TMP.

Effect of NO_3^-, HA, isopropanol, and WSP matrix

The effect of NO_3^- and organic matter, represented by HA, on the photolysis kinetics of antibiotics in an aqueous solution were investigated, and the resulting kinetic constants for the first and second order models are presented in Table S3 (SI section). The results indicated that the degradation of the antibiotics followed pseudo-first-order kinetics, with R^2 values of at least 0.96, while much lower values were obtained for the second-order model. The pseudo-first-order kinetics suggests that the photolysis half-life time in the environment will be independent of the initial concentration of the antibiotics.

The constants (k) and half-life times ($t_{1/2}$) obtained in the presence of NO_3^- and HA changed considerably in relation to ultrapure water (Table 1). The $t_{1/2}$ of TMP dropped from 82.1 to 27.5 h in the presence of NO_3^- and to 11.2 h in the presence of HA. For SMX, $t_{1/2}$ dropped from 12.0 to 5.3 h and rose slightly to 12.7 h under the influence of NO_3^- and HA, respectively.

The percentage of TMP photodegraded in the presence of NO_3^- in relation to ultrapure water increased from 50 to 81% and to 100% in the presence of HA after 6000 kJ m^{-2} of accumulated dose (66 h) (Figure 2b). The influence of humic acid on the photolysis of SMX was irrelevant, while in the presence of NO_3^-, the difference in the percentage of photolysis was not as significant as for TMP. However, the presence of this photosensitizer improved the kinetics of SMX, as only 4000 kJ m^{-2} cumulative solar irradiation dose were necessary for total degradation, a 30% decrease in the exposure time to solar irradiation when compared to the absence of NO_3^-.

Photodegradation increased in the presence of these components due to an indirect photolysis process since both can induce the generation of ROS, that can react with the antibiotics, enhancing their degradation. Organic matter

Table 1. Solar photolysis kinetics constants (k) and half-life time ($t_{1/2}$) of SMX and TMP at pH 7.2 in ultrapure water, WSP samples, and in the presence of NO_3^-, HA, and isopropanol

Matrix	SMX			TMP		
	k / h^{-1}	$t_{1/2}$ / h	R^2	k / h^{-1}	$t_{1/2}$ / h	R^2
Ultrapure water	0.0576	12.0	0.9973	0.0084	82.1	0.9975
Ultrapure water + NO_3^-	0.1320	5.3	0.9858	0.0252	27.5	0.9901
Ultrapure water + HA	0.0547	12.7	0.9917	0.0621	11.2	0.9767
WSP	0.0243	28.5	0.9934	0.0083	82.9	0.9654
WSP + isopropanol	0.0245	28.2	0.9960	0.0067	103.1	0.9608

SMX: sulfamethoxazole; TMP: trimethoprim; WSP: waste stabilization pond; NO_3^-: nitrate; HA: humic acid; R^2: determination coefficient.

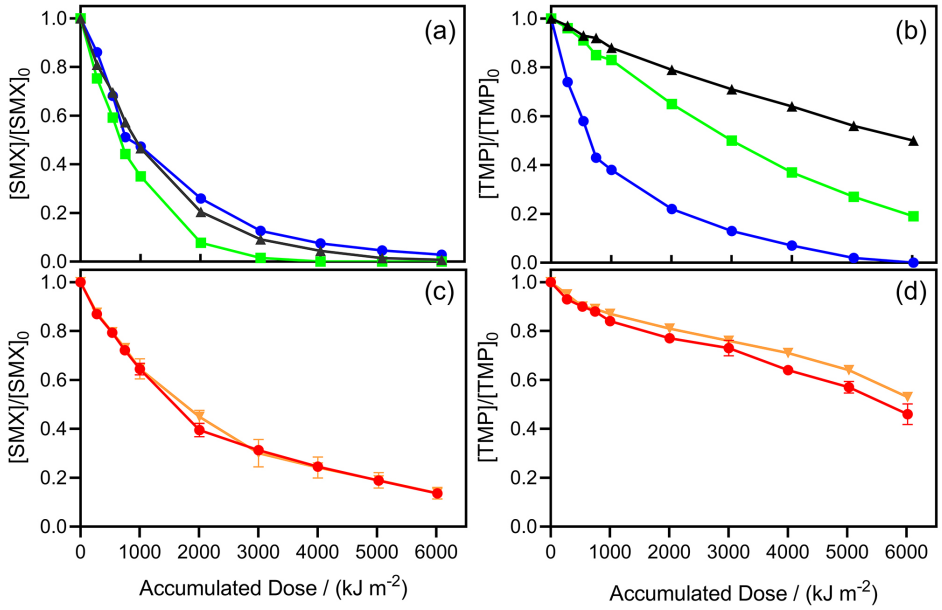

Figure 2. Effect of NO_3^- (-■-) and HA (-●-) in ultrapure water (-▲-) (a and b), and of isopropanol (-▼-) in Waste Stabilization Pond samples (-●-) (c and d) on solar photolysis of SMX and TMP. Conditions: 10 mg L^{-1} of NO_3^-, 143 mg L^{-1} of HA, 10 mmol L^{-1} of isopropanol and 500 µg L^{-1} of SMX and TMP at pH 7.2.

such as HA can be promoted to a transient excited state upon light absorption, which can either react directly with target compounds improving their photodegradation or with dissolved oxygen to form ROS (equations 3-7).[30,33,34] These reactive species then interact with target compounds. In addition, NO_3^- under radiation can also generate oxidizing species such as $HO^{\bullet}$ and $NO_3^{\bullet}$ (equation 8), which also participate in the process of indirect photolysis and increase the degradation of antibiotics.[33]

$$DOM \xrightarrow{hv} {}^1DOM^* \quad (3)$$

$$^1DOM^* \rightarrow {}^3DOM^* \quad (4)$$

$$^3DOM^* + \text{compounds} \rightarrow \text{products} \quad (5)$$

$$^3DOM^* + {}^3O_2 \rightarrow {}^1DOM + {}^1O_2 \quad (6)$$

$$^3DOM^* + {}^3O_2 \rightarrow DOM^{+\bullet} + O_2^{-\bullet} \quad (7)$$

$$NO_3^- \rightarrow^{hv} NO_3^{\bullet} \xrightarrow{hv} NO_2^{\bullet} + O^{-\bullet} \xrightarrow{H_2O} NO_2^{\bullet} + HO^- + HO^{\bullet} \quad (8)$$

Since these components are present in the WSP samples, it is important to investigate the occurrence of indirect photolysis in the matrix. For this purpose, experiments were performed with the addition of a well-known $HO^{\bullet}$ scavenger, isopropanol, in WSP samples. It was verified that the presence of isopropanol did not significantly affect the photolysis of SMX (Figure 2c). However, the photolysis of TMP was affected by the presence of isopropanol (Figure 2d), resulting in a $t_{1/2}$ increase from 82.9 h to 103.1 h (Table 1).

Considering the $t_{1/2}$ and the photodegradation percentages of the antibiotics, the photolysis of TMP was shown to be much more influenced by the presence of the photosensitizers and isopropanol than the photolysis of SMX.

The results in this study are consistent with the results of Ryan *et al.*[13] who studied the photolysis process of SMX and TMP and concluded that while 48% of the photodegradation of SMX in wastewater effluent occurred due to a direct process, for TMP the direct photolysis is responsible for only 18% of its photodegradation, the removal of this antibiotic occurred mostly by photosensitizers, with $HO^{\bullet}$ accounting for 62%, and triplet excited effluent organic matter for 20% of the photolysis of this drug. Other previous studies[27,28,31,35] also demonstrated this behavior of the antibiotics, while SMX is photodegraded mainly by direct photolysis, the TMP direct photolysis is slower and more easily photodegraded in the presence of photosensitizers.

As evidenced by Luo *et al.*[36] direct photolysis depends on the molecular structure, which in the case of SMX it is likely related to the multiple dissociation sites in the bonds with $–NH_2–$, –S–, –NH–, –N–O–. Additionally, the conjugated double bonds of the isoxazole ring and between the S and O atoms in SMX facilitate $\pi \rightarrow \pi^*$ transition reactions that have low absorption energy, which increases the absorptivity of the compound.[36] However, as shown by Jodeh *et al.*[37] the negative electronic chemical potential of TMP structure provides the molecule more stability.

The structural differences between the two molecules also influence the energy gap between the HOMO and LUMO orbitals. While the gap between $E_{HOMO} - E_{LUMO}$ of TMP is 5.258 eV, the SMX gap is 4.94 eV. A larger gap between $E_{HOMO} - E_{LUMO}$ value results in higher absorption energy for TMP and a slower photolysis reaction rate, while SMX with a smaller gap value has a higher reaction rate.[36,37]

In addition, SMX has a strong phosphorescent characteristic, with maximum emission at 410 nm, which denotes that it can form excited triplet states in contrast to TMP. The presence of excited triplet states is an indicator of photochemical reactivity, which justifies the greater potential of SMX to participate in photochemical reactions in contrast to TMP, which shows higher persistence under irradiation.[28]

When evaluating the matrix effect, only the photolysis of SMX was affected in WSP samples (Figure 3). Compared with the results shown in Figure 1, the pH had a greater influence on the photolysis of antibiotics than the water matrix. The photolysis of both antibiotics followed a pseudo-first-order kinetic model and the $t_{1/2}$ of SMX increased from 12.0 to 28.5 h in WSP samples (Table 1). However, $t_{1/2}$ of TMP was not significantly affected by the matrix and no significant difference in the degradation percentages, kinetic constants, and $t_{1/2}$ were observed. The dark controls showed less than 10% decrease in SMX concentration after 6000 kJ m^{-2} and even lower in the case of TMP, indicating negligible hydrolysis or biodegradation.

Under controlled conditions, with the addition of photosensitizers in ultrapure water, the photolysis was favored (Figure 2), but in the WSP matrix, opposite results were observed because of the complexity of this matrix, besides NO_3^- and HA. For example, species such as chloride and carbonate can scavenge $HO^{\bullet}$, which would hinder the indirect photolysis, while the higher turbidity of the WSP samples may also affect photodegradation.[4,33] The mechanisms involved in the photolysis of drugs in matrices such as WSP are not fully understood since several simultaneous reactions can contribute to the degradation process and even hinder the photodegradation of micropollutants.[4,33]

Considering that the main goal of this study was to evaluate whether the photolysis of these antibiotics can occur naturally during their residence time in WSP and prevent the discharge of these drugs to the aquatic environment, the maximum period that the antibiotics can be exposed to solar irradiation during the time they remain in the WSP was estimated based on the residence time in the WSP of 41 h.

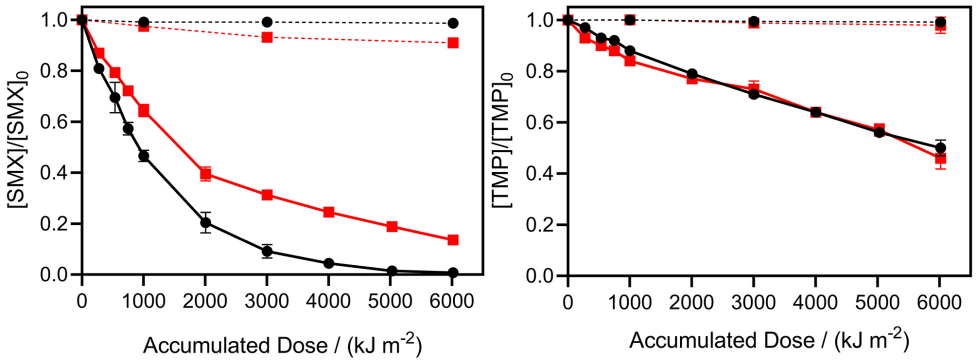

Figure 3. SMX and TMP solar photolysis in ultrapure water (-●-) and Waste Stabilization Pond samples (-■-). Dashed lines: dark control experiments. Conditions: pH 7.2; 500 μg L^{-1} of SMX and TMP.

In the best-case scenario, between the months of November and January, the daily insolation in the site is at least 13 h (Figure S4, SI section). Considering the residence time at this WSP, the antibiotics are exposed to solar irradiation for a maximum of 26 h. Considering the $t_{1/2}$ value of 28.5 and 82.9 for SMX and TMP, respectively (Table 1), 26 h is not enough to reach 50% removal of any of the antibiotics, demanding a longer residence time in the WSP to provide higher degradation. Under these conditions, it is expected that SMX and TMP would be discharged in the form of photoproducts as well as unaltered molecules.

Photoproducts identification

To evaluate the generated photoproducts, the antibiotics were irradiated separately in ultrapure water. The photoproducts were analyzed using LC-MS/MS and their structures were elucidated by comparing them to literature data (formula, retention times and times of irradiation are shown in Table S4, SI section, and the *m/z* of photoproducts fragments are shown in Table S5, SI section).

For TMP, eight photoproducts have been identified (Figure 4) that have already been determined in previous studies[31,35,38,39] and are formed by carbonylation, hydroxylation, and demethylation mechanisms during the photodegradation process. Since HO• radicals are nonselective, three isomers were also detected (*m/z* 323, P5, P6, and P7) as well as in a previous study.[35] In addition, no product of bond cleavage was detected in this study.

The photoproducts of P2 (*m/z* 307), P3 (*m/z* 339), and the three isomers P5, P6, and P7 (*m/z* 323) are the result of direct hydroxylation of TMP. The photoproducts P4 (*m/z* 325) and P8 (*m/z* 305) were obtained by carbonylation of the pyridine ring and the methylene group, respectively. Photoproduct P1 (*m/z* 309), on the other hand, is the result of demethylation followed by hydroxylation.[38,39]

All photoproducts of the TMP remained present in the solution even after more than 70 h of exposure to solar irradiation, indicating their resistance to photolysis. However,

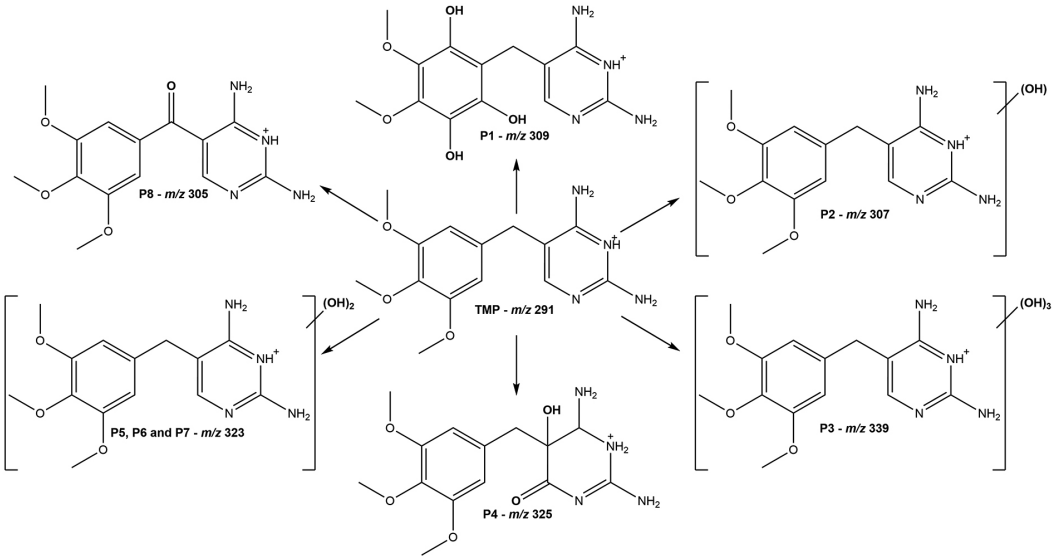

Figure 4. Photoproducts identified during the photolysis of TMP: structures and *m/z* of the protonated ions. Conditions: 500 μg L^{-1} of SMX; pH 7.2.

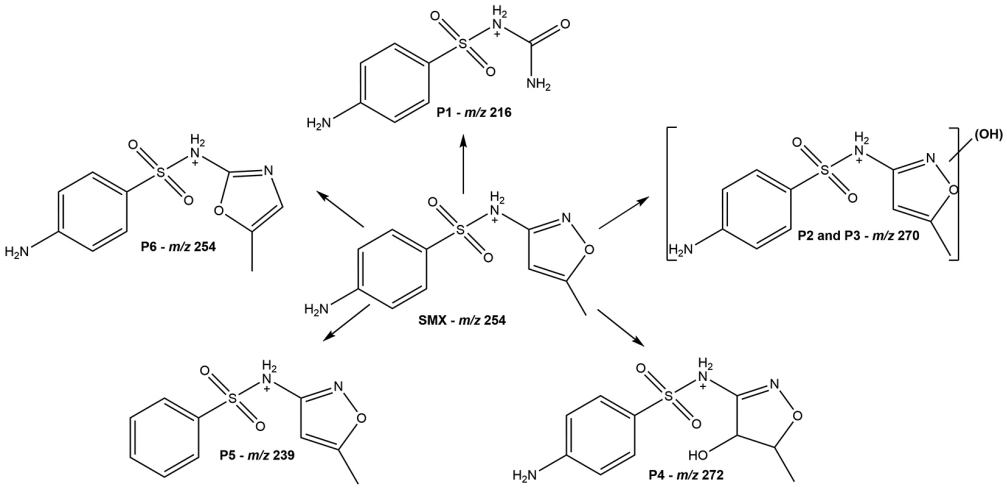

Figure 5. Photoproducts identified during the photolysis of SMX: structures and *m/z* of the protonated ions. Conditions: 500 μg L^{-1} of SMX; pH 7.2.

previous studies[38,39] have demonstrated that none of the photoproducts identified in this work possess significant toxicity, suggesting a low risk to aquatic environment.

Six SMX photoproducts detected (Figure 5) have already been found in previous studies. Among them, P1 (*m/z* 216) was obtained after opening the isoxazole ring,[40] the P2 and P3 isomers (*m/z* 270) resulted from the hydroxylation reactions,[41,42] P4 (*m/z* 272) after breaking the double bond of the isoxazole ring and hydroxylation,[40] P5 (*m/z* 239) resulting from the loss of the NH_2 group during photolysis [43] and P6 (*m/z* 254), which is an isomer of SMX, obtained by rearrangement of the isoxazole ring.[9,40,43]

Disinfection

Considering the importance of disinfection in WWTP, which could be achieved during irradiation, the quantification of pathogens was performed in the samples collected at WSP, before and after exposure to natural solar irradiation to evaluate if exposure during the residence time in the WSP would lead to pathogen inactivation.

All target microorganisms, total and thermotolerant coliforms and *Escherichia coli*, were decreased to concentrations below the LOQ (1 CFU *per* 100 mL) after 6000 kJ m^{-2} of accumulated solar energy, while in the dark controls, the decrease was much lower, proving that total inactivation was due to exposure to solar irradiation and showing the effectiveness of natural solar irradiation to reduce the microbial load in WSP (Figure 6).

In summary, exposure of microorganisms to solar irradiation can lead to internal cellular damage of these pathogens by two main routes. The first involves deoxyribonucleic acid (DNA) damage by direct absorption of radiation. In the second, the absorption of light by the pathogen promotes an excess formation of intracellular ROS that through various reactions causes lethal damage to the microorganism leading to its inactivation.[3,44] In more complex matrices with the presence of photosensitizers, such as organic matter, microbial inactivation can also occur through the generation of HO$^{\bullet}$ and other oxidizing species in the medium. These species can act as disinfectants and contribute to the inactivation of pathogens.[45]

Although this study has demonstrated that total disinfection of WSP effluent by solar radiation occurs, it

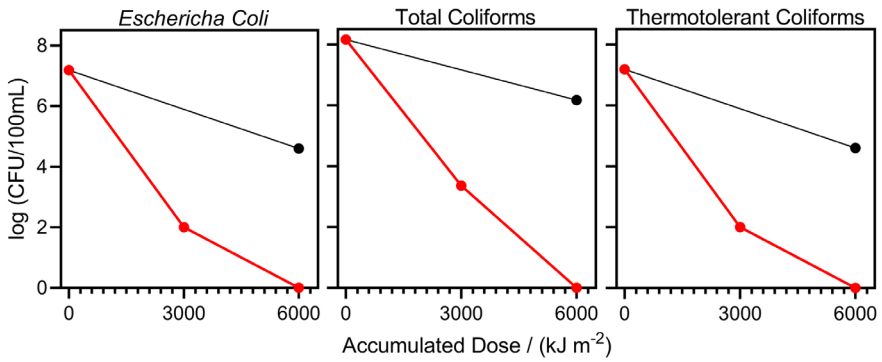

Figure 6. Inactivation of *Escherichia coli*, total coliforms, and thermotolerant coliforms in Waste Stabilization Ponds samples by solar photoinactivation (–●–), and control in the dark (–●–).

is important to note that it was achieved after 14 days of experimentation (average of 5.5 h of daily sun exposure), while the residence time of the effluent in the WWTP is only 1.7 days (41 h), insufficient to achieve total disinfection. Previous studies[46,47] comparing the results of solar irradiation disinfection with solar irradiation disinfection combined with photo-Fenton also showed slower or incomplete inactivation of bacteria applying solar irradiation alone.

Conclusions

The presence of NO_3^- and HA increased the indirect photolysis of TMP, since both induce ROS generation, while SMX was less influenced since it is more susceptible to direct photolysis. However, the natural solar photolysis of both antibiotics in WSP samples was impaired, due to the presence of other matrix components that can scavenge oxygen species and hinder the penetration of light. Studies in the presence of the $HO^{\bullet}$ scavenger isopropanol showed that $HO^{\bullet}$ did not play a relevant role in the indirect photolysis of the SMX, but slightly affected TMP due to its greater tendency to undergo indirect photolysis than SMX. SMX and TMP photolysis were shown to be notably more affected by pH than by the WSP matrix. The exposure of the antibiotics SMX and TMP to solar irradiation in WSP can promote their photolysis and enable disinfection of the matrix. However, considering the degradation kinetics obtained and the residence time in the WSP (41 h), it is possible to conclude that solar photolysis under these conditions is not sufficient to provide total photodegradation of antibiotics and disinfection of the effluent in the WSP.

Supplementary Information

Supplementary information is available free of charge at http://jbcs.sbq.org.br as PDF file.

Acknowledgments

The authors are grateful to the Coordination for the Improvement of Higher Education Personnel (CAPES) for a doctoral scholarship awarded to Karla Virginia Leite Lima (Code 001), DAAE/Araraquara for providing the Waste Stabilization Pond samples and Dr Ian Castro Gamboa for making available the MS analysis. The authors also thank the São Paulo Research Foundation, for support of this work and a postdoctoral fellowship awarded to Jany Hellen Ferreira de Jesus (FAPESP grants 2018/12780-4 and 2019/22218-4).

Author Contributions

Karla V. L. Lima was responsible for conceptualization, methodology, formal analysis, investigation, writing-original draft, review and editing, visualization; Jany H. F. de Jesus for methodology, formal analysis, investigation, writing-original draft, review and editing, visualization; João L. Bronzel Junior for methodology, formal analysis, writing original draft; Raquel F. P. Nogueira for conceptualization, methodology, writing-review and editing, supervision, project administration, funding acquisition.

References

1. Gruchlik, Y.; Linge, K.; Joll, C.; *J. Environ. Manage.* **2018**, *206*, 202. [Crossref]
2. Ragush, C. M.; Poltarowicz, J. M.; Lywood, J.; Gagnon, G. A.; Hansen, L. T.; Jamieson, R. C.; *Ecol. Eng.* **2017**, *98*, 91. [Crossref]
3. Ho, L.; Goethals, P. L. M.; *Ecol. Eng.* **2020**, *148*, 105791. [Crossref]
4. Guo, Z.; Kodikara, D.; Albi, L. S.; Hatano, Y.; Chen, G.; Yoshimura, C.; Wang, J.; *Water Res.* **2022**, 118236. [Crossref]
5. Michael, I.; Rizzo, L.; McArdell, C. S.; Manaia, C. M.; Merlin, C.; Schwartz, T.; Dagot, C.; Fatta-Kassinos, D.; *Water Res.* **2013**, *47*, 957. [Crossref]
6. Wang, Y.; Roddick, F. A.; Fan, L.; *Chemosphere* **2017**, *185*, 297. [Crossref]
7. Silva, C. P.; Oliveira, C.; Ribeiro, A.; Osório, N.; Otero, M.; Esteves, V. I.; Lima, D. L. D.; *Chemosphere* **2020**, *238*, 124613. [Crossref]
8. Liang, C.; Zhao, H.; Deng, M.; Quan, X.; Chen, S.; Wang, H.; *J. Environ. Sci.* **2015**, *27*, 115. [Crossref]
9. Gmurek, M.; Horn, H.; Majewsky, M.; *Sci. Total Environ.* **2015**, *538*, 58. [Crossref]
10. Kang, Y.-M.; Kim, M.-K.; Zoh, K.-D.; *Chemosphere* **2018**, *204*, 148. [Crossref]
11. Lastre-Acosta, A. M.; Barberato, B.; Parizi, M. P. S.; Teixeira, A. C. S. C.; *Environ. Sci. Pollut. Res.* **2019**, *26*, 4337. [Crossref]
12. Li, Y.; Qin, H.; Li, Y.; Lu, J.; Zhou, L.; Chovelon, J. M.; Ji, Y.; *Water Res.* **2021**, *200*, 117275. [Crossref]
13. Ryan, C. C.; Tan, D. T.; Arnold, W. A.; *Water Res.* **2011**, *45*, 1280. [Crossref]
14. Pereira, E.; Martins, F.; Gonçalves, A.; Costa, R.; Lima, F.; Rüther, R.; Abreu, S.; Tiepolo, G.; Pereira, S.; Souza, J.; *Atlas Brasileiro de Energia Solar*, 2nd ed.; INPE: São José dos Campos, 2017.
15. von Sperling, M.; *Urban Wastewater Treatment in Brazil*; IDB: Washington, 2016. [Link] accessed in November 2023
16. Arsand, J. B.; Hoff, R. B.; Jank, L.; Bussamara, R.; Dallegrave, A.; Bento, F. M.; Kmetzsch, L.; Falção, D. A.; Peralba, M. C. R.; Gomes, A. A.; Pizzolato, T. M.; *Sci. Total Environ.* **2020**, *738*, 139781. [Crossref]

17. Bisognin, R. P.; Wolff, D. B.; Carissimi, E.; Prestes, O. D.; Zanella, R.; *Environ. Technol.* **2021**, *42*, 2292. [Crossref]
18. Böger, B.; Surek, M.; Vilhena, R. O.; Fachi, M. M.; Junkert, A. M.; Santos, J. M.; Domingos, E. L.; Cobre, A. F.; Momade, D. R.; Pontarolo, R.; *J. Hazard. Mater.* **2021**, *402*, 123448. [Crossref]
19. Gomes, M. P.; Brito, J. C. M.; Vieira, F.; Kitamura, R. S. A.; Juneau, P.; *Front. Environ. Sci.* **2022**, *9*, 1. [Crossref]
20. Danner, M. C.; Robertson, A.; Behrends, V.; Reiss, J.; *Sci. Total Environ.* **2019**, *664*, 793. [Crossref]
21. Hiller, C. X.; Hübner, U.; Fajnorova, S.; Schwartz, T.; Drewes, J. E.; *Sci. Total Environ.* **2019**, *685*, 596. [Crossref]
22. Qiao, M.; Ying, G. G.; Singer, A. C.; Zhu, Y. G.; *Environ. Int.* **2018**, *110*, 160. [Crossref]
23. Vikesland, P. J.; Pruden, A.; Alvarez, P. J. J.; Aga, D.; Bürgmann, H.; Li, X. D.; Manaia, C. M.; Nambi, I.; Wigginton, K.; Zhang, T.; Zhu, Y.-G.; *Environ. Sci. Technol.* **2017**, *51*, 13061. [Crossref]
24. Departamento Autônomo de Água e Esgotos (DAAE), https://daaeararaquara.com.br/esgoto/, accessed in October 2023.
25. de Jesus, J. H. F.; Lima, K. V. L.; Pupo Nogueira, R. F.; *J. Environ. Chem. Eng.* **2022**, *10*, 107765. [Crossref]
26. American Public Health Association (APHA); *Standard Methods for the Examination of Water and Wastewater*, 22nd ed.; American Water Works Association (AWWA): Washington, 2012.
27. Boreen, A. L.; Arnold, W. A.; McNeill, K.; *Environ. Sci. Technol.* **2004**, *38*, 3933. [Crossref]
28. Zhou, W.; Moore, D. E.; *J. Photochem. Photobiol., B* **1997**, *39*, 63. [Crossref]
29. Asghar, A.; Lutze, H. V.; Tuerk, J.; Schmidt, T. C.; *J. Hazard. Mater.* **2022**, *429*, 128189. [Crossref]
30. Oliveira, C.; Lima, D. L. D.; Silva, C. P.; Calisto, V.; Otero, M.; Esteves, V. I.; *Sci. Total Environ.* **2019**, *648*, 1403. [Crossref]
31. Luo, X.; Zheng, Z.; Greaves, J.; Cooper, W. J.; Song, W.; *Water Res.* **2012**, *46*, 1327. [Crossref]
32. Baeza, C.; Knappe, D. R. U.; *Water Res.* **2011**, *45*, 4531. [Crossref]
33. Ribeiro, A. R. L.; Moreira, N. F. F.; Li Puma, G.; Silva, A. M. T.; *Chem. Eng. J.* **2019**, *363*, 155. [Crossref]
34. Torres-Palma, R. A.; Serna-Galvis, E. A.; Ávila-Torres, Y. P. In *Nano-Materials as Photocatalysts for Degradation of Environmental Pollutants: Challenges and Possibilities*; Singh, P.; Borthakur, A.; Mishra, P. K.; Tiwary, D., eds.; Elsevier: Amsterdam, 2019, p. 211-243.
35. Sirtori, C.; Agüera, A.; Gernjak, W.; Malato, S.; *Water Res.* **2010**, *44*, 2735. [Crossref]
36. Luo, S.; Wei, Z.; Spinney, R.; Zhang, Z.; Dionysiou, D. D.; Gao, L.; Chai, L.; Wang, D.; Xiao, R.; *J. Hazard. Mater.* **2018**, *343*, 132. [Crossref]
37. Jodeh, S.; Jaber, A.; Hanbali, G.; Massad, Y.; Safi, Z. S.; Radi, S.; Mehmeti, V.; Berisha, A.; Tighadouini, S.; Dagdag, O.; *BMC Chem.* **2022**, *16*, 17. [Crossref]
38. Michael, I.; Hapeshi, E.; Osorio, V.; Perez, S.; Petrovic, M.; Zapata, A.; Malato, S.; Barceló, D.; Fatta-Kassinos, D.; *Sci. Total Environ.* **2012**, *430*, 167. [Crossref]
39. Zhang, N.; Zhou, B.; Yuan, R.; Wang, F.; Chen, H.; *Water* **2020**, *12*, 2935. [Crossref]
40. Trovó, A. G.; Nogueira, R. F. P.; Agüera, A.; Sirtori, C.; Fernández-Alba, A. R.; *Chemosphere* **2009**, *77*, 1292. [Crossref]
41. Segalin, J.; Arsand, J. B.; Jank, L.; Schwalm, C. S.; Streit, L.; Pizzolato, T. M.; *Sci. Total Environ.* **2022**, *828*, 154109. [Crossref]
42. Willach, S.; Lutze, H. V.; Eckey, K.; Löppenberg, K.; Lüling, M.; Wolbert, J. B.; Kujawinski, D. M.; Jochmann, M. A.; Karst, U.; Schmidt, T. C.; *Environ. Sci. Technol.* **2018**, *52*, 1225. [Crossref]
43. Bonvin, F.; Omlin, J.; Rutler, R.; Schweizer, W. B.; Alaimo, P. J.; Strathmann, T. J.; McNeill, K.; Kohn, T.; *Environ. Sci. Technol.* **2013**, *47*, 6746. [Crossref]
44. Giannakis, S.; Polo López, M. I.; Spuhler, D.; Sánchez Pérez, J. A.; Fernández Ibáñez, P.; Pulgarin, C.; *Appl. Catal., B* **2016**, *199*, 199. [Crossref]
45. McGuigan, K. G.; Conroy, R. M.; Mosler, H. J.; du Preez, M.; Ubomba-Jaswa, E.; Fernandez-Ibañez, P.; *J. Hazard. Mater.* **2012**, *235-236*, 29. [Crossref]
46. Rodríguez-Chueca, J.; Polo-López, M. I.; Mosteo, R.; Ormad, M. P.; Fernández-Ibáñez, P.; *Appl. Catal., B* **2014**, *150-151*, 619. [Crossref]
47. Ndounla, J.; Spuhler, D.; Kenfack, S.; Wéthé, J.; Pulgarin, C.; *Appl. Catal., B* **2013**, *129*, 309. [Crossref]

Submitted: July 26, 2023
Published online: November 9, 2023